JB
Journals.ASM.org

Derepression of the *Bacillus subtilis* PerR Peroxide Stress Response Leads to Iron Deficiency

Melinda J. Faulkner,* Zhen Ma, Mayuree Fuangthong,* and John D. Helmann

Department of Microbiology, Cornell University, Ithaca, New York, USA

The *Bacillus subtilis* PerR repressor regulates the adaptive response to peroxide stress. The PerR regulon includes the major vegetative catalase (*katA*), an iron storage protein (*mrgA*), an alkylhydroperoxide reductase (*ahpCF*), a zinc uptake system (*zosA*), heme biosynthesis enzymes (*hemAXCDBL*), the iron uptake repressor (*fur*), and *perR* itself. A *perR* null strain is resistant to hydrogen peroxide, accumulates a porphyrin-like compound, and grows very slowly. The poor growth of the *perR* mutant can be largely accounted for by the elevated expression of two proteins: the KatA catalase and Fur. Genetic studies support a model in which poor growth of the *perR* null mutant is due to elevated repression of iron uptake by Fur, exacerbated by heme sequestration by the abundant catalase protein. Analysis of the altered-function allele *perR991* further supports a link between PerR and iron homeostasis. Strains containing *perR991* are peroxide resistant but grow nearly as well as the wild type. Unlike a *perR* null allele, the *perR991* allele (F51S) derepresses KatA, but not Fur, which likely accounts for its comparatively rapid growth.

Iron is an essential element used as a cofactor for numerous enzymes in nearly all cells. Iron-containing proteins typically include those with mononuclear iron centers, iron-sulfur clusters, or heme (1). Iron is often limiting for growth in natural environments, such as the soil or ocean, due to its low solubility under aerobic conditions. As a result, bacteria have developed numerous mechanisms to obtain iron, including the synthesis of high-affinity chelators (siderophores) and a variety of iron uptake transporters (2). Pathogenic bacteria also require efficient iron acquisition mechanisms that allow them to grow within the iron-restricted environment of the host (16, 57). The expression and activity of high-affinity iron uptake systems must be tightly regulated to prevent internalization of excess iron, which can lead to production of toxic free radicals. Specifically, ferrous iron [Fe(II)] can react with hydrogen peroxide (H_2O_2), generating hydroxyl radical, hydroxide anion, and oxidized ferric iron [Fe(III)] in the Fenton reaction (42, 43). The highly reactive hydroxyl radical can damage DNA and proteins, leading to mutations and, ultimately, cell death.

In most bacteria, iron uptake systems are conditionally expressed in response to iron limitation. The most widespread mechanism of regulation involves an iron-activated DNA-binding repressor known as Fur (ferric uptake repressor) (23, 47). The *Bacillus subtilis* Fur regulon includes ~40 proteins expressed in response to iron deprivation and the small regulatory RNA (sRNA) FsrA (4, 27). The derepressed proteins include enzymes for the synthesis of bacillibactin (a catecholate siderophore), several ABC transporters for the import of ferric-bacillibactin and other ferric-siderophore complexes, two flavodoxins, and additional proteins with uncertain relevance to iron homeostasis (28, 52, 54, 58). The derepression of the FsrA sRNA and three coregulated accessory proteins (FbpA, FbpB, FbpC) serves to downregulate low-priority iron-utilizing enzymes in times of iron deficiency (27).

In addition to Fur, *Bacillus subtilis* encodes two Fur paralogs with distinct metal-sensing properties (56). The Zur repressor senses Zn(II) and serves to regulate zinc homeostasis in a manner analogous to that of Fur (29, 31, 50). The PerR repressor senses peroxide stress (21, 67). PerR associated with either Mn(II) or Fe(II) (PerR:Mn and PerR:Fe, respectively) can repress transcription, but only PerR:Fe senses H_2O_2 (46, 51). The PerR-repressed genes encode the major vegetative catalase (*katA*), a miniferritin iron storage protein (*mrgA*), a peroxidase (alkylhydroperoxide reductase, *ahpCF*), a zinc uptake system (*zosA*), heme biosynthesis enzymes (*hemAXCDBL*), the ferric uptake repressor (*fur*), and *perR* itself (22, 38) (Fig. 1). PerR also plays an auxiliary role in regulating expression of *spx* (48), which coordinates the disulfide stress response, and positively regulates the *srfA* operon, which encodes enzymes for surfactin biosynthesis (36).

PerR requires a bound regulatory metal ion in order to bind DNA (39). As a result, the PerR regulon can be derepressed when cells are grown under conditions depleted for both iron and manganese (14). Under most growth conditions, PerR is in its Fe(II)-liganded form and is highly sensitive to H_2O_2. Reaction with peroxides results in metal-catalyzed protein oxidation, leading to the formation of 2-oxo-histidine and the loss of bound iron (46). This leads to derepression of PerR-regulated genes. Conversely, when iron is limiting and manganese is abundant, PerR is in an Mn(II)-liganded state and represses the PerR regulon, even in the presence of H_2O_2 (14, 26). Thus, the ability of H_2O_2 to derepress the PerR regulon is sensitive to the Fe(II)/Mn(II) ratio in the cell (22). One poorly understood complexity of the PerR regulon is that the extent of peroxide responsiveness varies among regulon members (26) (Fig. 1). This may be due to variations in the affinities of the PerR:Fe and PerR:Mn forms of PerR for various operator sites.

Received 22 November 2011 **Accepted** 16 December 2011

Published ahead of print 22 December 2011

Address correspondence to John D. Helmann, jdh9@cornell.edu.

* Present address: Melinda J. Faulkner, Department of Biology, Bradley University, Peoria, Illinois, USA; Mayuree Fuangthong, Laboratory of Biotechnology, Chulabhorn Research Institute, Lak Si, Bangkok, Thailand.

Supplemental material for this article may be found at http://jb.asm.org/.

doi:10.1128/JB.06566-11

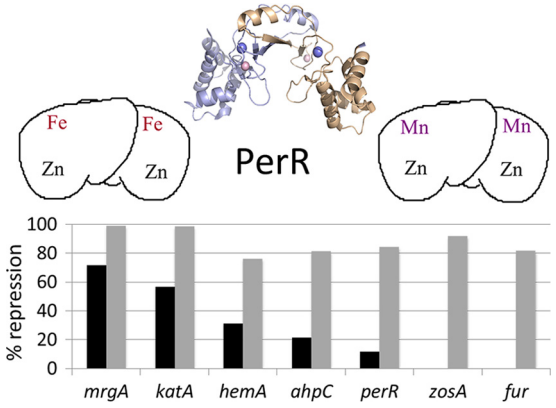

FIG 1 Metal dependence of repression of PerR regulon genes. The structure of the dimeric PerR repressor is shown (44), with bound metal ions indicated as spheres. This is flanked by schematic diagrams illustrating the two distinct functional forms, PerR:Fe and PerR:Mn. Both forms contain a structural Zn(II) ion (46) together with a regulatory metal ion. As described previously, only the PerR:Fe form responds to H_2O_2 under physiologically relevant conditions. The bottom panel illustrates the differential abilities of Fe(II) (black bars) and Mn(II) (gray bars) to repress various PerR target operons, as monitored by β-galactosidase assays. Cells were resuspended in defined minimal medium lacking added iron and containing a minimal amount of Mn(II) to support growth. Gene expression under these derepressing conditions was measured after 3 h. When cells were instead resuspended in medium containing either 10 μM Fe(II) or 5 μM Mn(II), gene expression was reduced (measured as % repression) as noted (adapted from Fig. 4A in reference 26). Note that Mn(II) is an effective corepressor for all PerR regulon genes, whereas Fe(II)-mediated repression efficiency decreases from left to right (with little or no repression observed for *perR*, *zosA*, and *fur*).

Collectively, these results support a model in which PerR links regulation of the peroxide stress response with iron homeostasis. This link is further strengthened by the observation that the PerR regulon includes Fur itself, KatA (an abundant heme-containing catalase), and the MrgA iron storage protein (12, 26).

As previously reported, a *B. subtilis* strain lacking *perR* grows very slowly in nonstressed conditions and readily forms faster-growing isolates that often lack catalase activity (11). Furthermore, the *perR* strain produces a pink-pigmented compound. However, the reason for the slow-growth phenotype has not been defined. Here, we investigate the pleiotropic phenotype of the *perR* mutant strain and provide evidence that poor growth results from gross perturbations in iron homeostasis due to the combined effects of elevated levels of Fur and KatA.

MATERIALS AND METHODS

Bacterial strains and growth conditions. All strains, unless indicated otherwise, are derivatives of the wild-type (WT) CU1065 (Table 1). *B. subtilis* cells were grown in LB medium or metal-limited minimal (MM) medium prepared with ultrapure filter-sterilized metal stocks and Chelex-treated (Chelex 100 Resin, Bio-Rad) and filter-sterilized stocks of all non-metal-containing components. MM medium contains 40 mM potassium morpholinepropanesulfonic acid (MOPS) (adjusted to pH 7.4 with KOH), 2 mM potassium phosphate buffer (pH 7.0), glucose (2% wt/vol), $(NH_4)_2SO_4$ (2 g/liter), $MgSO_4 \cdot 7H_2O$ (0.2 g/liter), potassium glutamate (1 g/liter), tryptophan (10 mg/liter), and 80 nM $MnCl_2$, similar to that described previously (32). Metals and trisodium citrate-dihydrate (1 g/liter) from filter-sterilized stocks were added before inoculation. Metals and trisodium citrate-dihydrate were also added to LB medium when indicated. Metals were added at the indicated concentrations, and citrate was added at a concentration of either 1 g/liter or twice that of the added iron. Liquid cultures were incubated at 37°C with shaking at 200 rpm. Growth curves were determined by using a Bioscreen C machine (Growth Curves USA).

The colony size of a given strain was determined by picking a fresh colony from an LB agar plate, resuspending the colony in LB medium, and diluting and spreading the cell suspension on an LB agar plate to result in the formation of well-isolated colonies (~30 to 300 colonies/plate). The diameters of isolated colonies were measured using a ruler while they were viewed under a stereo microscope. Twenty-five colonies were measured for each strain to determine its average colony size (reported in mm).

Routine molecular biology procedures were done as described by

TABLE 1 Strains used in this study

B. subtilis strain	Genotype	Reference or source
CU1065	W168 *att*SPβ *trpC2*	Laboratory stock
HB2078	CU1065 *perR*::*kan*	26
HB2194	CU1065 *perR*::*spc*	25
HB9703	CU1065 *perR*::*tet*	Laboratory stock
HB2162	CU1065 $katA_{\Delta 355-483}$(*erm*) (*katA355*)	3
HB14109	CU1065 *katA*::*mls* (null mutation)	This study
HB14108	CU1065 $kat_{E218stop}$-*cat*	This study
HB14107	CU1065 *katA-cat* ("wild-type" *katA*)	This study
HB2163	CU1065 *mrgA*::*cat*	Laboratory stock
HB1703	CU1065 *ahpC*:Tn*10*(*spc*)	Laboratory stock
HB8103	CU1065 *zosA*::*kan*	30
HB2165	CU1065 *perR*::*kan* $katA_{\Delta 355-483}$(*erm*)	Laboratory stock
HB14113	CU1065 *perR*::*spc katA*::*mls*	This study
HB14117	CU1065 *perR*::*spc* $katA_{E218stop}$-*cat*	This study
HB14116	CU1065 *perR*::*spc katA-cat*	This study
HB14067	CU1065 *perR*::*spc mrgA*::*cat*	This study
HB14070	CU1065 *perR*::*kan ahpC*::Tn*10*(*spc*)	This study
HB14071	CU1065 *perR*::*spc zosA*::*kan*	This study
HB2501	CU1065 *fur*::*kan*	4
HB14092	CU1065 *fur*::*kan fsrA*::*cat*	27
HB14009	CU1065 *perR*::*spc fur*::*kan*	This study
HB14010	CU1065 *perR*::*spc fur*::*kan fsrA*::*cat*	This study
HB14082	CU1065 *perR*::*spc* P_{spac}-*hemAXCDBL*	This study
HB14121	CU1065 *perR*::*spc mrgA*::*cat katA*::*mls*	This study
HB14123	CU1065 *perR*::*spc fur*::*kan katA*::*mls*	This study
HB5612	CU1065 *yfmC*::*mls*	58
HB14091	CU1065 *perR*::*spc fur*::*kan yfmC*::*mls*	This study
HB5624	CU1065 *feuA*::*spc*	58
HB5608	CU1065 *fhuB*::*mls*	58
HB5610	CU1065 *yusV*::*mls*	58
HB5606	CU1065 *yhfQ*::*cat*	58
HB5604	CU1065 *yclN*::*mls*	58
HB5622	CU1065 *ywbL*::*cat*	58
HB5620	CU1065 *ywjA*::*spc*	58
YB886	*trpC2 metB5 xin-1* SPβ	35
MA991	YB886 containing *perR991*(*F51S*) allele	35
ZB307A	W168 SPβ*c2*Δ*2*::Tn*917*::pSK10Δ*6*	68
HB14031	CU1065 *perR*::*spc thrC*::*perR*	This study
HB14032	CU1065 *perR*::*spc thrC*::*perR991*	This study
HB0518	ZB307A SPβ*c2*Δ*2*::Tn*917*::Φ(*katA′-cat-lacZ*)	26
HB2083	CU1065 SPβ*c2*Δ*2*::Tn*917*::Φ(*ahpC′-lacZ*)	26
HB1122	ZB307A SPβ*c2*Δ*2*::Tn*917*::Φ(*mrgA′-cat-lacZ*)	26
HB1041	CU1065 *hemA′-lacZ*	14
HB2076	CU1065 SPβ*c2*Δ*2*::Tn*917*::Φ(*fur′-cat-lacZ*)	26
HB8108	CU1065 SPβ*c2*Δ*2*::Tn*917*::Φ(*zosA′-cat-lacZ*)	26
HB2062	CU1065 SPβ*c2*Δ*2*::Tn*917*::Φ(*perR′-cat-lacZ*)	26
HB14102	CU1065 *perR*::*spc* P_{spac}-*fur*	This study
HB14103	CU1065 *amyE*::P_{spac}-*fur*	This study

Sambrook et al. (63). Isolation of *B. subtilis* chromosomal DNA, transformation, and specialized SPβ transduction were done as described previously (18). Restriction enzymes (New England BioLabs), DNA ligase (New England BioLabs), and DNA polymerase (Bio-Rad, Thermo Scientific, and Roche) were used in accordance with the manufacturer's instructions. *B. subtilis* strains were constructed using long-flanking homology PCR, as described in Butcher and Helmann (10). Antibiotics were added as follows for selection: 1 μg/ml erythromycin and 25 μg/ml lincomycin (for selecting for macrolide-lincosamide-streptogramin B [MLS] resistance), 100 μg/ml spectinomycin, 8 μg/ml chloramphenicol, 10 μg/ml kanamycin, 5 μg/ml tetracycline, and 10 μg/ml neomycin.

Escherichia coli DH5α was used for routine DNA cloning as described in Sambrook et al. (63). Ampicillin was used at a concentration of 100 μg/ml for selection of plasmids in *E. coli*. The P_{spac}-*hemAXCDBL* allele was constructed by cloning a fragment of the *hemA* gene into the vector pMUTIN4 using the primers *hemA*-fwd-HindIII (5′-CGTAGCAAGCTT GTTGGGGGTGTAATTAGAGCG) and *hemA*-rev-BamHI (5′-CGCAC AGGATCCGAGAATCAATATGTGCTTGC) (64). The *hemA* fragment was amplified by PCR. Both *hemA′* and pMUTIN4 were digested with the restriction enzymes HindIII and BamHI, ligated using T4 DNA ligase, and transformed in DH5α. The resulting plasmid was then transformed into *B. subtilis*. The P_{spac}-*fur* allele was constructed similarly but used primers *fur*-fwd-HindIII (5′-CATGGAAAGCTTCGTAGGAGGGAAAGACA TGG) and *fur*-int-rev-BamHI (5′-GTCGTGGGATCCGCCCTCTTTCC GAAGGTC) to amplify *fur*. The *amyE*::P_{spac}-*fur* allele was constructed similarly, but it used the primers *fur*-fwd-HindIII and *fur*-rev-BglII (5′-G CTGTGAGATCTGGTTCCAGTTATATAAACCATATGCC) and was cloned into the vector pPL82 (61). The resulting plasmid was linearized by digestion with PvuI prior to transformation into *B. subtilis*. The resulting constructs were induced using the indicated concentration of isopropyl-β-D-thiogalactopyranoside (IPTG).

The *katA* E218stop-cat allele was constructed by cloning a fragment of the *katA* gene into the vector pGEM-cat using primers *katA*-int-fwd-KpnI (5′-CCTGTCGGTACCCTTTCTGAAGTCGGCAAACGC) and *katA*-218stop-rev-SphI (5′-CGTCAGGCATGCTTATGTTTTAAAG TGATATTTAATCCATACGCC). A control wild-type *katA* allele was constructed similarly but used the primer *katA*-rev-SphI (5′-CGACTGG CATGCGATGAGAAGCATACGCAATGTGTAAC). The *katA* fragments and pGEM-cat (26) were digested with the restriction enzymes KpnI and SphI, ligated using T4 ligase, and transformed into DH5α. The resulting plasmids were used to transform *B. subtilis* to chloramphenicol resistance.

The *thrC*::*perR* and *thrC*::*perR991* alleles were constructed by amplifying the wild-type *perR* allele from CU1065 or the *perR991* allele from MA991, both containing their native promoter sequences, using the primers *perR*-prom-fwd-BamHI (5′-GACTGTGGATCCTATGAGCCTATGC CTACTTTTACCCTG) and *perR*-rev-EcoRI (5′-CGACGCGAATTCAG CTGACCGTTTCGTGCG). The vector pDG1664 (33) and the *perR* alleles were digested with the restriction enzymes BamHI and EcoRI, ligated using T4 ligase, and transformed into DH5α. The resulting plasmids were linearized by digestion with PvuI and used to transform *B. subtilis*.

Catalase activity. Cells were grown on LB agar plates overnight. A colony was picked from the fresh plate and placed in a drop of dilute hydrogen peroxide. Strains resulting in the formation of bubbles were determined to possess catalase activity. For quantitative determinations of catalase activity, cells were assayed for the rate of H_2O_2 decomposition spectrophotometrically (240 nm), as described previously (5).

Porphyrin purification and thin-layer chromatography (TLC) analysis. C_{18} resin (Supelco) was used to partially purify porphyrins from the supernatants using methods similar to those described previously (24, 59). Briefly, strains were grown overnight in LB medium containing 2% xylose (to enhance porphyrin accumulation). Ten milliliters of the supernatants from these cultures was loaded onto 50 mg of prepared C_{18} resin (washed with methanol and then water) by mixing the resin and supernatant in a microcentrifuge tube, pelleting the resin, and removing the remaining supernatant. The resin was then washed once with water and once with 20% acetone. Porphyrins were eluted using 200 μl of 100% acetone. The supernatant from a 250-ml culture of the *perR*::*kan* strain was purified using a similar procedure but with a C_{18} column. Eluted fractions exhibiting a bright pink color were kept for porphyrin analysis.

The C_{18}-purified supernatants and porphyrin standards (in 100% acetone) were analyzed using thin-layer chromatography (TLC) as described previously (24, 59). Briefly, approximately 5 μl of the compounds was spotted onto silica gel plates. The mobile phase consisted of *N*,*N*-dimethylformamide, methanol, ethylene glycol, acetic acid, 1-chlorobutane, and chloroform in a ratio of 4:35:6:0.4:18:20 (vol/vol/vol/vol/vol/vol). Porphyrins were visualized by UV light and photographed using a digital camera. Uroporphyrin III dihydrochloride (MP Biomedicals, LLC), coproporphyrin III dihydrochloride (CPIII; MP Biomedicals, LLC), and protoporphyrin IX (Sigma-Aldrich) dissolved in acetone were used as standards.

β-Galactosidase activity assays. Overnight cultures of cells grown in LB medium were transferred at a 1:100 dilution into fresh LB medium for β-galactosidase activity assays,. The cells were grown to an optical density at 600 nm (OD_{600}) of 0.6. All assays were performed on triplicate samples, and the values were averaged. β-Galactosidase activity was measured using a modification of the previously described method of Miller (13, 55).

UV-visible and fluorescence spectroscopy. The C_{18}-purified supernatant in 10 mM Tris, pH 8.0, was added to a quartz cuvette, and the UV-visible spectra were determined from 230 nm to 700 nm. The excitation ($\lambda_{em} = 581$ nm) and emission ($\lambda_{ex} = 402$ nm) spectra were measured with the C_{18}-purified supernatant and coproporphyrin III (CPIII) in 10 mM Tris, pH 8.0.

Electrospray ionization-tandem mass spectrometry. Electrospray ionization-tandem mass spectrometry (ESI-MS/MS) of the C_{18}-purified supernatant and CPIII was performed with the compounds in a 3:1 mixture of methanol/1% formic acid (vol/vol) and analyzed using MassLynx software.

Whole-genome resequencing. Chromosomal DNA from $perR_{supp}$ strains was prepared using the Qiagen DNeasy blood and tissue kit. The DNA was sequenced and analyzed by the Cornell University Life Sciences Core Laboratories Center using Illumina DNA sequencing.

Cellular iron content measurement by ICP-MS. Four milliliters of mid-log-phase cells was harvested and washed once with phosphate-buffered saline (PBS) buffer containing 1 mM nitrilotriacetic acid, followed by two PBS buffer-only washes. Cells were then resuspended in 400 μl PBS buffer, from which 50 μl was used for an OD_{600} measurement. Ten microliters of 10 mg/ml lysozyme was added to the remaining cells and incubated at 37°C for 20 min. Six hundred microliters 5% HNO_3 with 0.1% (vol/vol) Triton X-100 was then added, and the samples were boiled at 95°C for 30 min. Samples were then centrifuged, and the supernatants were diluted for inductively coupled plasma mass spectrometry (ICP-MS) measurements. All samples were analyzed using the Perkin Elmer ELAN DRC II ICP-MS, equipped with a Microflow PFA-ST nebulizer. The DRC mode was used with ammonia as the reaction gas. Gallium was added at 50 ppb as an internal standard by an in-line mixing block. The total concentrations of metal ions were calculated assuming 5.9×10^8 cells/OD_{600} (41) and a cell volume of 1.0×10^{-14} liters/cell (53).

Quantification of Fur by a Western blot. A sample of 5 ml of mid-log-phase cells was harvested and lysed by addition of 10 μl of 10 mg/ml lysozyme and sonication in 20 mM Tris [pH 8.0], 0.1 M NaCl, and 1 mM dithiothreitol (DTT). After centrifugation, the total soluble protein concentration was determined by a Bradford assay using bovine serum albumin (BSA) as a standard. A Western blot was performed as described, with the exception that a 1:1,000 dilution of rabbit antiserum raised against *B. subtilis* Fur was used as the primary antibody (8). Known amounts of purified Fur protein were loaded for quantification (8). Multiple samples with different amounts of cell extracts and purified Fur proteins were loaded for better quantification.

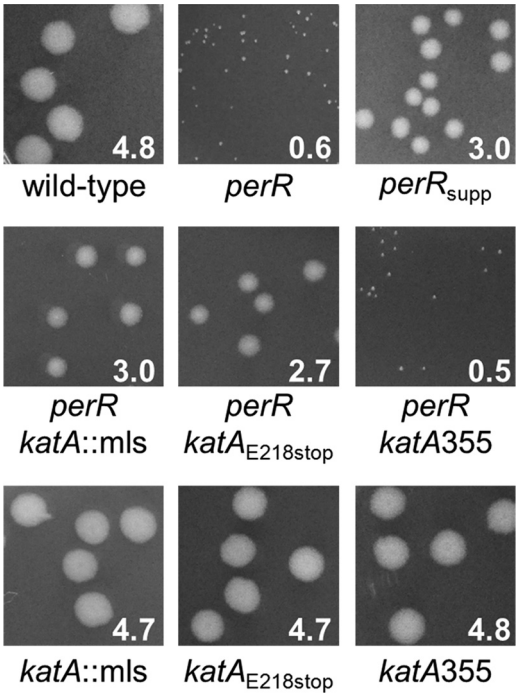

FIG 2 Effects of catalase mutations on growth of the *perR* strain. The first row compares growth of the wild-type strain, a *perR* null mutant, and a typical spontaneous suppressor strain. The second row illustrates the ability of *katA* null alleles to suppress the poor growth of the *perR* null mutation (with the exception of *katA355*; see text). The third row demonstrates that the *katA* alleles have little measurable effect on growth in the wild-type background. In this and subsequent figures, the numbers in the lower right corner of each picture indicate the average colony size (in mm) of 25 isolated colonies after growth on LB agar at 37°C for 24 h. In all cases, the standard deviation of these measurements was less than 10% of the reported value.

RESULTS AND DISCUSSION

Derepression of the PerR regulon negatively affects cell growth. A *perR* null mutant strain grows very slowly and has a substantial decrease in colony size on LB agar (Fig. 2), consistent with previous reports (9). Expression of *perR* from an ectopic locus restores wild-type growth. Additionally, the *perR* null strain frequently forms fast-growing isolates (*perR*$_{supp}$). To determine the frequency of these suppressor mutations, we picked small colonies of the *perR* strain from LB agar, resuspended them in LB broth, and plated serial dilutions of the suspensions on LB agar plates. We counted the number of CFU after 1 day (representing the faster-growing variants containing suppressor mutations) and the total number of CFU after 2 days. We found that a significant fraction of the resulting colonies (~0.3%) contained one or more suppressor mutations. Due to this high frequency of suppressor formation, we were unable to obtain reliable measurements of growth rates for the *perR* strain in liquid cultures. Instead, we routinely measured colony diameters after 24 h of growth of suitably diluted cultures on LB plates.

Loss of catalase activity correlates with an improved growth rate of the *perR* mutant strain. As noted previously, ~80% of the *perR*$_{supp}$ strains lack catalase activity (11). Since the gene encoding the major vegetative catalase (*katA*) is derepressed in a *perR* mutant (9), we speculated that the suppressor mutations may be null mutations of *katA*. Therefore, the *katA* regions in four of the *perR*$_{supp}$ strains that lacked catalase activity were sequenced. Three of these strains were found to contain a partial deletion of *katA*. In the fourth strain, a point mutation results in a stop codon at position 218. Three of the *perR*$_{supp}$ strains that retained catalase activity were also sequenced and, as expected, contain wild-type *katA*.

To test whether elimination of *katA* is sufficient to restore good growth to the *perR* strain, we transformed a *perR* null mutation into a strain (HB2162) containing a previously described *katA* null mutation (3). Although this strain lacks catalase activity, this *katA* allele was not sufficient to improve growth (Fig. 2). We subsequently noted that this allele (*katA355*), which was constructed by Campbell integration, may still express a truncated protein containing the first 355 amino acids (~73%) of the native coding sequence. We speculate that this protein, which retains the complete heme-binding pocket according to the structure of *Enterococcus faecalis* catalase (34) (see Fig. S1 in the supplemental material), may still bind heme and thereby contribute to the poor growth of the *perR* mutant. In contrast, strains with true null mutations of *katA*, including either an allelic replacement that eliminates the *katA* coding sequence (*katA*::*mls*) or the *katA*$_{E218stop}$ allele, significantly improve growth of the *perR* strain (Fig. 2).

The poor growth of the *perR* mutant is largely due to derepression of KatA and Fur. Since only some of the *perR*$_{supp}$ strains contained mutations in *katA*, and since deletion of *katA* in the *perR* strain only partially restored growth, we reasoned that overproduction of one or more of the other PerR target genes (Fig. 1) might also contribute to poor growth. First, we tested *mrgA*, which encodes a miniferritin predicted to sequester iron (15). However, a *perR mrgA* strain still grew poorly (Fig. 3). Similarly, derepression of *ahpC* (7) and *zosA* (30) also does not appear to contribute significantly to the poor-growth phenotype of *perR* (Fig. 3).

In contrast with these results, a *perR fur* double mutant strain grew significantly better than *perR* (Fig. 3), and complementation with *fur*, as described in Materials and Methods, again led to very poor growth (data not shown). This suggests that iron homeostasis may be disrupted in the *perR* strain as a result of derepression of Fur. Next, we constructed the triple mutant *perR katA fur*. The effects of the *fur* and *katA* mutations are additive with respect to growth, and the triple mutant grows nearly as well as the wild-type strain (Fig. 3). We conclude that the poor-growth phenotype of the *perR* null mutant can be largely accounted for by the derepression of KatA (which sequesters heme iron) and Fur (which perturbs iron homeostasis).

The dramatic effects of KatA on growth of the *perR* mutant are consistent with previous data suggesting that catalase is a highly expressed protein. Previous measurements of KatA activity in wild-type cells suggest that this protein is normally present at ~0.3% of the total cell protein and that total activity increases ~30-fold after peroxide induction (49). We have noted previously that in the *perR* null strain, KatA is a major band easily detected by Coomassie blue staining of whole-cell extracts (12, 14). We therefore quantified KatA by Coomassie blue staining of whole-cell extracts and determined the level in a *perR fur* double mutant (to avoid accumulation of suppressors lacking catalase). Similar levels of catalase were found in both logarithmic- and stationary-phase cells: in both cases, catalase is the single most abundant protein and represents ~10% of the total cell protein by weight (see Fig. S2 in the supplemental material).

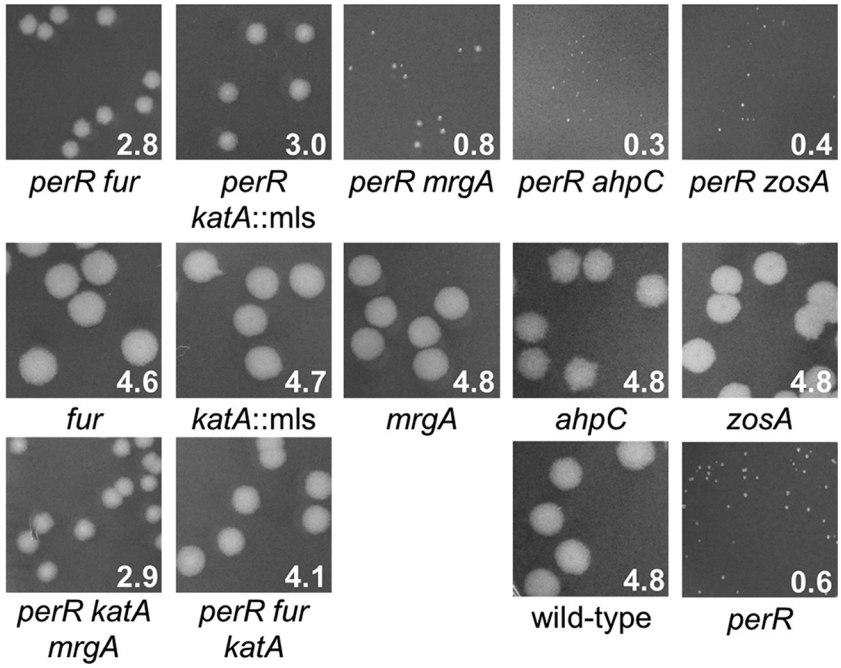

FIG 3 Effects of mutations in PerR target genes on growth of the *perR* strain. Growth measurements (as for Fig. 2) indicate that mutations in *fur* and *katA* suppress the poor growth of the *perR* strain, whereas mutations in *mrgA*, *ahpC*, and *zosA* do not (WT and *perR* null mutant controls are shown in the lower right). The panels in the second row demonstrate that these mutations have little effect on growth in the wild-type background. The third row illustrates that *katA* and *fur* are additive with respect to growth, whereas *katA* and *mrgA* are not.

Fur protein impairs growth by repression of iron uptake. The iron-loaded Fur protein regulates iron homeostasis through two main mechanisms: by the repression of iron uptake functions and by the indirect activation of iron-requiring enzymes (by repression of the inhibitory FsrA sRNA). As shown previously (27), many of the pleiotropic growth phenotypes of a *fur* mutant are due to FsrA, which translationally represses expression of iron-containing metabolic enzymes. We therefore hypothesized that this FsrA-mediated repression in the *perR fur* double mutant might account for the improved growth relative to that of the *perR* single mutant. However, a *perR fur fsrA* strain grew as well as a *perR fur* strain. Thus, the ability of a *fur* mutation to improve the growth of the *perR* mutant is not due to derepression of *fsrA* (Fig. 4).

We next hypothesized that the ability of the *fur* mutation to improve growth of the *perR* strain is due to the derepression of one or more of the Fur-regulated iron transport systems (58). Therefore, we individually transformed null mutations in each of the Fur-regulated iron transporter systems into the *perR fur* strain and assessed the effect on growth on LB agar. However, none of the resulting triple mutant strains showed a significant growth defect (data not shown), suggesting that multiple transporters are responsible for improved growth on this medium. *B. subtilis* 168 strains, including the WT strain CU1065 used here, are known to be defective in the synthesis of bacillibactin, the catecholate siderophore made by many natural isolates of *B. subtilis*. In the absence of siderophore synthesis, iron uptake relies largely on the YfmCDEF iron-citrate uptake system in medium containing citrate and on the YwbLMN elemental iron uptake system in medium lacking citrate (58). Indeed, these two systems appear to play redundant roles for iron uptake on LB medium, since the *perR fur ywbL yfmC* quadruple mutant, much like the *perR* mutant, forms very small colonies (Fig. 4). A *yfmC ywbL* double mutant strain is somewhat reduced in growth, even in a *fur* background (Fig. 4). These results suggest that mutation of *fur* improves growth of the *perR* null mutant by allowing the expression of two partially redundant high-affinity iron uptake systems. This further implies that high-affinity iron uptake systems are important during colony growth, even on an iron-rich medium like LB.

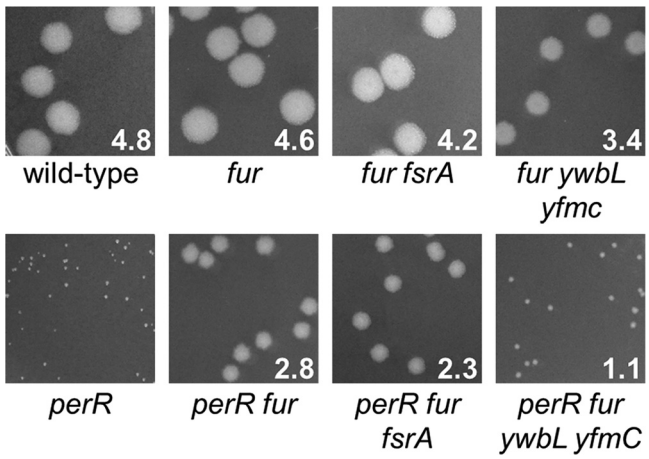

FIG 4 The *perR* strain is defective for iron import. Growth measurements (as for Fig. 2) shown in the second row indicate that the ability of a *fur* mutation to improve the growth of a *perR* null mutant is not due to derepression of FsrA but requires the presence of the *ywbLMN* and *yfmCDEF* operons encoding elemental iron and ferric citrate uptake systems, respectively (58). The first row demonstrates that these two uptake systems contribute to growth even in a wild-type background.

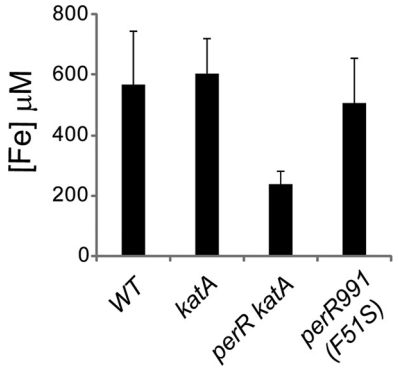

FIG 5 A *perR* null mutant has reduced cellular iron content. Iron content was monitored in the wild-type strain, a *katA* null, a *perR katA* null, and the *perR991* strain by ICP-MS. A *perR* null strain was not used in these studies due to the complications of very poor growth and the resultant accumulation of suppressor mutations.

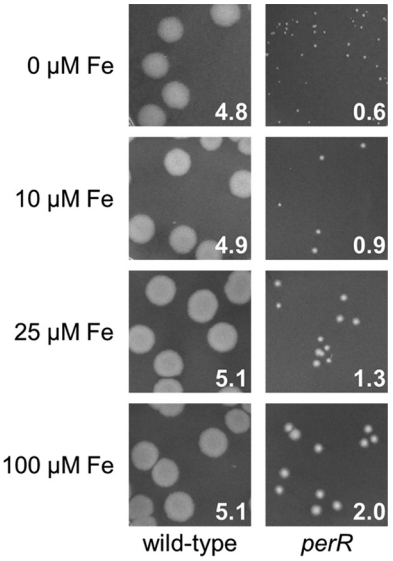

FIG 6 High levels of iron partially suppress the poor growth of the *perR* null mutant. Growth was measured on LB agar containing citrate and iron ($FeCl_3$) at 37°C for 24 h. Citrate was added to a concentration twice that of the iron.

To directly monitor the effects of PerR on iron homeostasis, we have used ICP-MS to quantify total intracellular iron in the wild type, a *katA* null mutant, and a *perR katA* double mutant. The WT and *katA* null cells had similar levels of total iron which were equivalent to an average intracellular concentration of ~560 μM. This is reduced to ~240 μM in the *perR katA* double mutant (Fig. 5). This large drop is primarily due to repression of iron uptake, although the level of heme iron associated with catalase is also significant. Based on our measurements of catalase levels, we predict that this single protein may sequester ~50 μM or ~20% of the total iron in the *perR* null mutant. This is consistent with the observation that mutation of either *katA* or *fur* increases growth of the *perR* mutant and that these two effects are additive. We conclude that the growth defect of the *perR* mutant strain is likely due to iron starvation. In support of this model, the addition of 100 μM $FeCl_3$ [but not Zn(II) or Mn(II)] to LB medium marginally improves growth of the *perR* strain (Fig. 6 and data not shown). We note that rescue by added iron is relatively inefficient and requires very high iron concentrations, presumably because the iron uptake systems are not expressed and this effect requires uptake through other, adventitious pathways.

A *perR* mutant has elevated levels of the Fur protein. Normally, Fur-mediated repression requires a bound Fe(II) cofactor and this binding interaction reports on iron sufficiency in the cell; when iron is limiting, Fur is inactive and import functions are expressed. In contrast, in the *perR* mutant strain, Fur seems to constitutively repress iron uptake. Since *fur* is itself regulated by *perR*, we hypothesized that the inability of cells to appropriately derepress iron uptake might be due to elevated Fur expression. Quantification of the Fur protein in both the wild-type strain and a *perR katA* null mutant indicates that Fur is unusually abundant for a regulatory protein. We estimate ~10,000 monomers of Fur per cell in the wild type, and this amount increases ~2.2-fold in the *perR* null mutant (see Fig. S3 in the supplemental material). This is consistent with the observation that a *fur-lacZ* transcriptional fusion is ~3-fold derepressed in a *perR* mutant (26). Relatively high levels of Fur protein have also been noted in *E. coli* (5,000 per cell during exponential growth and 10,000 per cell under oxidative stress) (66) and *Vibrio cholerae* (5,000 per cell) (65).

To test whether overproduction of Fur protein was, by itself, sufficient for repression of the Fur regulon, we constructed strains carrying an IPTG-inducible copy of *fur* integrated at *amyE* (*amyE*::P_{spac}-*fur*). In either a wild-type or a *fur*::*kan* genetic background, induction of Fur by the addition of 25 μM IPTG resulted in the inability of this strain to grow on LB agar (data not shown). Thus, overproduction of Fur can be toxic to cells even in the absence of PerR regulon derepression.

It is not immediately apparent why an increase in Fur concentration should grossly perturb the regulation of iron uptake since, *a priori*, we expected that Fur activity would still respond normally to Fe(II) levels in the cell. One possibility is that elevated Fur levels act, by mass action, to effectively lower the threshold level of Fe(II) needed to effect repression. Alternatively, changes in Fur protein levels may change the biochemical mechanism of ligand activation. For example, we recently reported that the ligand responsiveness of the related metalloregulator Zur can be altered by changes in protein concentration, at least *in vitro* (50). In the specific case of Zur, activation of DNA binding occurs by the stepwise binding of Zn(II) to a regulatory site in each protomer of the dimer. Since Zn(II) binding occurs with negative cooperativity, the dimeric repressor initially binds one regulatory Zn(II), and the second site is occupied only at higher Zn(II) concentrations. The first binding event only partially activates Zur to bind DNA, but at elevated concentrations of the Zur protein, this binding is sufficient to fully activate DNA binding (50). It is therefore possible that a similar scenario may pertain to iron activation of Fur; normally, activation requires multiple binding events that signal true iron sufficiency, whereas when Fur levels are elevated, the sensitivity to iron may increase and lead to repression of uptake, even when the cell is still—physiologically—iron deficient. Regardless of the underlying mechanism, our genetic results are consistent with the idea that, in the *perR* mutant background, Fur is present at an elevated level and now functions to repress iron uptake, even when cells are iron starved.

***perR* mutants accumulate a porphyrin-like compound.** In the course of these studies, we noted that the *perR* strain produces a pink-pigmented compound that accumulates in the supernatant

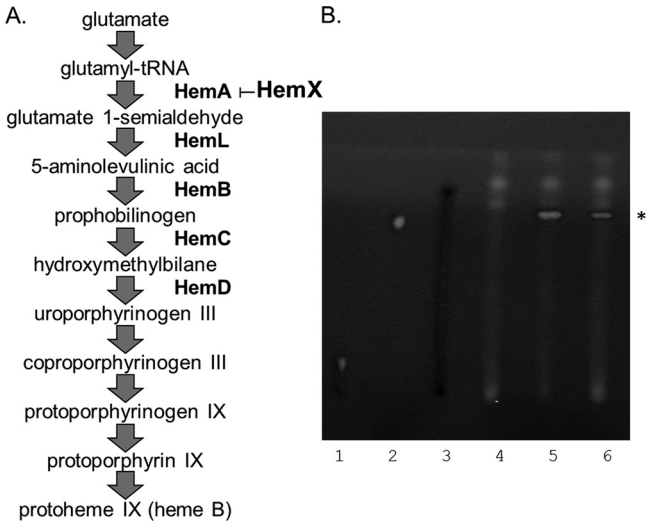

FIG 7 Accumulation of a porphyrin-like compound in *perR* and $perR_{supp}$ strains. (A) Heme biosynthesis pathway of *B. subtilis*, with enzymes regulated by PerR noted. (B) TLC of porphyrin standards (lanes 1 to 3) and C_{18}-purified supernatants from selected strains (lanes 4 to 6). Lane 1, uroporphyrinogen III; lane 2, CPIII; lane 3, protoporphyrin IX; lane 4, wild type; lane 5, *perR*; and lane 6, $perR_{supp}$. The asterisk indicates the position of the compound that accumulates in *perR* strains.

of liquid cultures. This pink color can also be seen on LB agar, and curiously, addition of either 2% xylose or 2% glucose increased production. Since the *hemAXCDBL* operon encoding the early steps in heme biosynthesis is repressed by PerR (Fig. 1), we reasoned that the pink compound may be a porphyrin. The enzymes HemAXCDBL synthesize uroporphyrinogen III from glutamate (Fig. 7A) (reviewed in reference 37). However, coproporphyrin III (CPIII), the subsequent intermediate in the biosynthesis pathway, is the precursor that accumulates most often in heme mutants (17, 45, 59). Chemical analyses are consistent with the notion that the accumulated compound is a novel tetrapyrrole which we designate as *TP*.

TP was purified from the supernatant of an overnight LB culture of the *perR* strain using C_{18} reverse-phase chromatography and analyzed by thin-layer chromatography (TLC). The mobility of *TP* during TLC is most similar to that of the CPIII standard (Fig. 7B). As expected, very little, if any, of the corresponding spot was visible in the supernatant fraction of wild-type cells. Characterization of *TP* by UV-visible and fluorescence spectroscopy reveals a number of striking similarities with CPIII (see Table S1 and Fig. S4 in the supplemental material). However, analysis of *TP* by electrospray ionization-tandem mass spectrometry (ESI-MS/MS) reveals two major species with *m/z* of 689 and 889 (see Fig. S5 in the supplemental material), neither of which correspond to that of CPIII (*m/z* 655). Furthermore, fragmentation of a CPIII standard requires a high collision energy (54 eV) and results in the cleavage of the side chain substituents (19). In contrast, fragmentation of *TP* required a much lower collision energy (27 eV) and resulted in the formation of a series of smaller fragment ions that differ by mass values of 228 Da, suggestive of a linear tetrapyrrole structure. The differences in UV-visible spectra, observed mass values, and fragmentation patterns lead us to conclude that *TP* is similar, but not identical, to CPIII and is likely a modified (and perhaps linear) tetrapyrrole.

We speculate that *TP* may be a modified and secreted porphyrin derivative produced in response to accumulation of CPIII (or other heme biosynthetic intermediates) in the *perR* mutant strain. Since heme biosynthesis is essential in *B. subtilis*, we were unable to test the requirement for heme biosynthesis genes using null mutants, as was done for other PerR regulon members. Instead, we decided to uncouple the expression of the *hemAXCDBL* operon from PerR activity using an IPTG-inducible P_{spac} promoter. Growth of a *perR* mutant strain containing P_{spac}-*hemAXCDBL* required the addition of at least 50 μM IPTG (data not shown). The production of the pink pigment was eliminated when the *hemA* operon was expressed from P_{spac}, even with 500 μM IPTG. Nevertheless, this strain still formed tiny colonies. Thus, the slow-growth phenotype of the *perR* mutant does not require the overproduction of porphyrins.

A *perR* missense mutant has increased peroxide resistance but maintains normal iron homeostasis. *B. subtilis* MA991 was previously isolated by serial passage into higher and higher levels of H_2O_2 (35). This strain expresses elevated levels of several PerR regulon members, including KatA, AhpCF, and MrgA. Yet, unlike a *perR* null mutant, strain MA991 grows nearly as well as the wild type. DNA sequence analysis revealed that MA991 carries an F51S missense allele of *perR* (*perR991*) (9) which alters a residue within the DNA-binding domain (44).

The fact that MA991 grows as well as its wild-type parent strain suggested that this strain might contain one or more suppressor mutations. To test this hypothesis, we complemented a *perR* null mutant by expressing *perR991* under its native promoter at the *thrC* locus. Introduction of *perR991* restored rapid growth to the *perR* null mutant, suggesting that *perR991* encodes a functional PerR protein. However, the complemented strain, like the *perR* null mutant, was still substantially more resistant to H_2O_2. We therefore hypothesized that *perR991* is an altered-function allele that somehow allows derepression of some or all of the PerR regulon without impeding cell growth.

We have demonstrated previously that there are differences in the patterns of regulation among PerR-regulated genes (26); some genes are preferentially repressed by PerR:Mn and not by PerR:Fe and, as a result, are poorly induced by H_2O_2 (Fig. 1). We therefore hypothesized that PerR991 might differentially affect the repression of various regulon members. To assess the ability of PerR991 to regulate genes in the PerR regulon, we analyzed transcriptional fusions of the various target genes to β-galactosidase (*lacZ*) in the *perR991* strain (Fig. 8). Consistent with the increased H_2O_2 resistance, both *katA* and *ahpC* were significantly derepressed in the *perR991* strain (29.1-fold and 3.2-fold, respectively, compared to 41.7-fold and 4.8-fold in the *perR* null strain). In contrast, the *mrgA* and *hemA* genes were only partially derepressed compared to their levels in the *perR* null strain (7.4-fold and 1.9-fold, respectively, for *perR991* compared to 140.4-fold and 6.6-fold for the *perR* null strain). The weak derepression of the *hemA* operon in the *perR991* strain is correlated with a greatly reduced accumulation of *TP*, as measured by TLC, relative to that in the null mutant (see Fig. S6 in the supplemental material). Interestingly, PerR991 not only still represses *fur* but also appears to repress *fur* slightly better than wild-type PerR (*fur* is repressed 1.7-fold in the *perR991* strain relative to wild-type expression, whereas it is derepressed by 2- to 3-fold in a *perR* null mutant) (Fig. 8). Consistent with this, the *perR991* strain appears to maintain normal iron homeostasis,

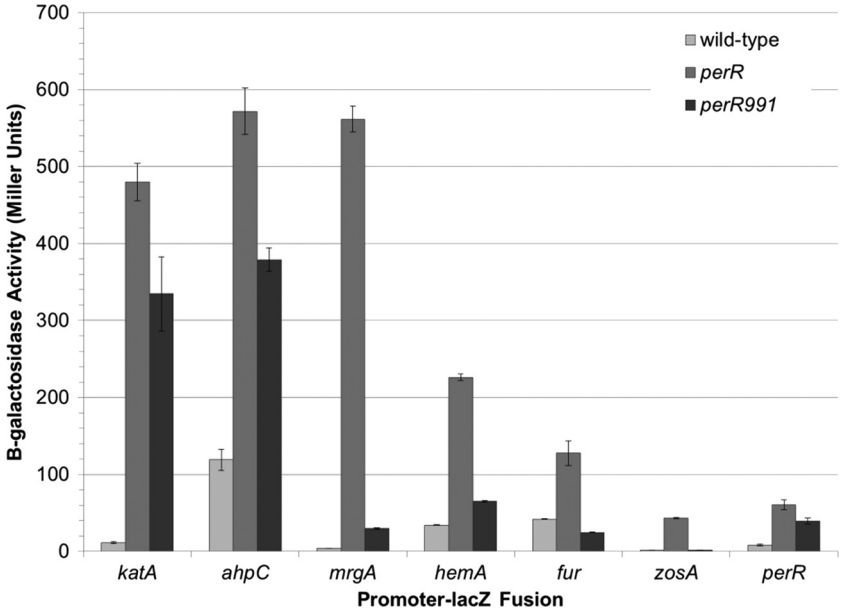

FIG 8 Repression of PerR regulon members in *perR991*. β-Galactosidase activity was determined for a *perR* null mutant complemented ectopically with wild-type *perR* (wild-type), $perR_{supp}$ (*perR*; representing the *perR* null parent strain), and the null strain complemented with the *perR991* allele. Strains were grown in LB at 37°C and contained transcriptional fusions of *lacZ* to the promoters of each *perR*-regulated operon as indicated.

as suggested by the total iron level, which is similar to that of WT cells (Fig. 5).

These results suggest that the PerR991 mutant protein may be altered in structure such that it is preferentially activated by Mn(II), a corepressor for the *fur* gene, while being defective in activation by Fe(II), the preferred corepressor for the *katA* and *ahpCF* operons (26). Indeed, mutations in the dimerization domain of PerR can alter the relative abilities of Fe(II) and Mn(II) to elicit repression (51). Alternatively, PerR991 may be altered in conformation such that the protein binds preferentially to those sites normally bound by PerR:Mn. This possibility is consistent with the observation that the F51S substitution is within the DNA-binding domain of PerR (44). Finally, this analysis indicates that overproduction of KatA does not, by itself, lead to poor growth. Instead, high levels of KatA exacerbate the severe iron starvation imposed on *perR* mutant cells by elevated Fur levels.

PerR and iron homeostasis are intimately linked. The observation that PerR functions as a metal-activated repressor of the peroxide stress response provided an early hint of the relationship between oxidative stress and iron homeostasis pathways (14). This link was further strengthened by the finding that PerR regulates heme biosynthesis, catalase, *fur* expression, and *mrgA*, which encodes a miniferritin that functions in iron storage (9, 12, 26). Here, we provide evidence that the *perR* strain is iron starved and that the resulting growth defect can be alleviated by the derepression of iron uptake pathways (controlled by Fur) and elimination of the heme sequestration activity of catalase. A slow-growth phenotype has been noted for some other *perR* null mutations, including *Listeria monocytogenes* (62), and we therefore note that genetic experiments that link mutations in *perR* to virulence defects must be interpreted with caution (6). Indeed, these defects may be due to iron starvation and poor growth. The relationships between PerR, Fur, and iron homeostasis are likely to be tuned to the biology of each organism. In the strict anaerobe *Clostridium acetobutylicum*, PerR appears to not affect cytosolic iron levels. Nevertheless, a *perR* null mutant grows more slowly anaerobically, but much better aerobically, than the wild type (40).

Although both Fur and KatA contribute to the poor growth of the *perR* null mutant, it is interesting to note that suppressors appear to arise preferentially in the *katA* gene. Indeed, mutations in *fur* have not been observed even in several suppressor strains that retain catalase activity. It is presently unclear whether this reflects a difference in spontaneous mutation frequencies within these two genes or whether the deleterious effects of the *fur* mutation on growth (largely due to FsrA-mediated effects [27]) contribute to this effect.

Our results also suggest questions that may guide future work. First, the nature of the tetrapyrrole compound that accumulates in the *perR* mutant is presently unknown. It was noted previously that the MA991 strain apparently secreted porphyrins (20) and that CPIII accumulates in iron-starved *B. subtilis* strains (60). Our preliminary chemical characterization suggests that this compound is related to CPIII but differs significantly in mass. One hypothesis is that cells that are overproducing heme precursors (due to derepression of the *hemAXCDBL* operon) but that are iron starved and unable to complete heme synthesis have a pathway to modify and excrete potentially toxic precursors. Second, this work again highlights the differences among PerR-regulated genes in metal responsiveness and, consequently, in peroxide inducibility (as summarized in Fig. 1). When *fur* was first shown to be repressed by PerR, we hypothesized that this might allow upregulation of Fur and, therefore, repression of iron uptake, when cells are exposed to reactive oxygen species (ROS). This would be analogous to the OxyR-mediated induction of *fur* shown in *E. coli* (66). However, we have yet to find a condition in which the *fur* gene is induced by peroxide stress (26). Instead, Fur expression seems to report on the relative levels of Mn(II) and Fe(II) in the cell. The physiological significance of this regulation and the mechanisms

underlying the differential regulation of PerR regulon genes await further investigation. Finally, the molecular basis for the constitutive repression of the Fur regulon despite apparent iron starvation is unclear. We note that the mechanism of iron activation of the Fur protein has not been resolved, and controversy lingers over the assignment and affinity of the metal-sensing site(s). It is anticipated that ongoing biochemical and genetic studies of Fur protein activation will help shed light on this unexpected regulatory phenomenon.

ACKNOWLEDGMENTS

We thank Anatol Eberhard for his help with the ESI-MS/MS analysis. We also thank previous lab members and visitors for their contributions to this project, including Ming Sun, Nakia M. Gray, Nada Bsat, and Jin-Won Lee.

This work was supported by a grant from the NIH (GM-059323).

REFERENCES

1. **Andreini C, Bertini I, Rosato A.** 2009. Metalloproteomes: a bioinformatic approach. Acc. Chem. Res. **42**:1471–1479.
2. **Andrews SC, Robinson AK, Rodriguez-Quinones F.** 2003. Bacterial iron homeostasis. FEMS Microbiol. Rev. **27**:215–237.
3. **Bagyan I, Casillas-Martinez L, Setlow P.** 1998. The *katX* gene, which codes for the catalase in spores of *Bacillus subtilis*, is a forespore-specific gene controlled by σ^F, and KatX is essential for hydrogen peroxide resistance of the germinating spore. J. Bacteriol. **180**:2057–2062.
4. **Baichoo N, Wang T, Ye R, Helmann JD.** 2002. Global analysis of the *Bacillus subtilis* Fur regulon and the iron starvation stimulon. Mol. Microbiol. **45**:1613–1629.
5. **Beers RF, Jr, Sizer IW.** 1952. A spectrophotometric method for measuring the breakdown of hydrogen peroxide by catalase. J. Biol. Chem. **195**: 133–140.
6. **Brenot A, King KY, Caparon MG.** 2005. The PerR regulon in peroxide resistance and virulence of *Streptococcus pyogenes*. Mol. Microbiol. **55**: 221–234.
7. **Bsat N, Chen L, Helmann JD.** 1996. Mutation of the *Bacillus subtilis* alkyl hydroperoxide reductase (*ahpCF*) operon reveals compensatory interactions among hydrogen peroxide stress genes. J. Bacteriol. **178**:6579–6586.
8. **Bsat N, Helmann JD.** 1999. Interaction of *Bacillus subtilis* Fur (ferric uptake repressor) with the *dhb* operator in vitro and in vivo. J. Bacteriol. **181**:4299–4307.
9. **Bsat N, Herbig A, Casillas-Martinez L, Setlow P, Helmann JD.** 1998. *Bacillus subtilis* contains multiple Fur homologues: identification of the iron uptake (Fur) and peroxide regulon (PerR) repressors. Mol. Microbiol. **29**:189–198.
10. **Butcher BG, Helmann JD.** 2006. Identification of *Bacillus subtilis* σ^W-dependent genes that provide intrinsic resistance to antimicrobial compounds produced by Bacilli. Mol. Microbiol. **60**:765–782.
11. **Casillas-Martinez L, Driks A, Setlow B, Setlow P.** 2000. Lack of a significant role for the PerR regulator in *Bacillus subtilis* spore resistance. FEMS Microbiol. Lett. **188**:203–208.
12. **Chen L, Helmann JD.** 1995. *Bacillus subtilis* MrgA is a Dps(PexB) homologue: evidence for metalloregulation of an oxidative-stress gene. Mol. Microbiol. **18**:295–300.
13. **Chen L, James LP, Helmann JD.** 1993. Metalloregulation in *Bacillus subtilis*: isolation and characterization of two genes differentially repressed by metal ions. J. Bacteriol. **175**:5428–5437.
14. **Chen L, Keramati L, Helmann JD.** 1995. Coordinate regulation of *Bacillus subtilis* peroxide stress genes by hydrogen peroxide and metal ions. Proc. Natl. Acad. Sci. U. S. A. **92**:8190–8194.
15. **Chiancone E, Ceci P.** 2010. The multifaceted capacity of Dps proteins to combat bacterial stress conditions: detoxification of iron and hydrogen peroxide and DNA binding. Biochim. Biophys. Acta **1800**:798–805.
16. **Chu BC, et al.** 2010. Siderophore uptake in bacteria and the battle for iron with the host; a bird's eye view. Biometals **23**:601–611.
17. **Cox R, Charles HP.** 1973. Porphyrin-accumulating mutants of *Escherichia coli*. J. Bacteriol. **113**:122–132.
18. **Cutting SM, Vander Horn PB.** 1990. Genetic analysis, p 27–74. *In* Harwood CR, Cutting SM (ed), Molecular biological methods for bacillus. John Wiley and Sons, Ltd., Chichester, United Kingdom.
19. **Danton M, Lim CK.** 2006. Porphyrin profiles in blood, urine and faeces by HPLC/electrospray ionization tandem mass spectrometry. Biomed. Chromatogr. **20**:612–621.
20. **Dowds BC.** 1994. The oxidative stress response in *Bacillus subtilis*. FEMS Microbiol. Lett. **124**:255–263.
21. **Duarte V, Latour JM.** 2010. PerR vs OhrR: selective peroxide sensing in *Bacillus subtilis*. Mol. Biosyst. **6**:316–323.
22. **Faulkner MJ, Helmann JD.** 2011. Peroxide stress elicits adaptive changes in bacterial metal ion homeostasis. Antioxid. Redox Signal. **15**:175–189.
23. **Fleischhacker AS, Kiley PJ.** 2011. Iron-containing transcription factors and their roles as sensors. Curr. Opin. Chem. Biol. **15**:335–341.
24. **Friedmann HC, Baldwin ET.** 1984. Reverse-phase purification and silica gel thin-layer chromatography of porphyrin carboxylic acids. Anal. Biochem. **137**:473–480.
25. **Fuangthong M, Helmann JD.** 2003. Recognition of DNA by three ferric uptake regulator (Fur) homologs in *Bacillus subtilis*. J. Bacteriol. **185**: 6348–6357.
26. **Fuangthong M, Herbig AF, Bsat N, Helmann JD.** 2002. Regulation of the *Bacillus subtilis fur* and *perR* genes by PerR: not all members of the PerR regulon are peroxide inducible. J. Bacteriol. **184**:3276–3286.
27. **Gaballa A, et al.** 2008. The *Bacillus subtilis* iron-sparing response is mediated by a Fur-regulated small RNA and three small, basic proteins. Proc. Natl. Acad. Sci. U. S. A. **105**:11927–11932.
28. **Gaballa A, Helmann JD.** 2011. *Bacillus subtilis* Fur represses one of two paralogous haem-degrading monooxygenases. Microbiology **157**:3221–3231.
29. **Gaballa A, Helmann JD.** 1998. Identification of a zinc-specific metalloregulatory protein, Zur, controlling zinc transport operons in *Bacillus subtilis*. J. Bacteriol. **180**:5815–5821.
30. **Gaballa A, Helmann JD.** 2002. A peroxide-induced zinc uptake system plays an important role in protection against oxidative stress in *Bacillus subtilis*. Mol. Microbiol. **45**:997–1005.
31. **Gaballa A, Wang T, Ye RW, Helmann JD.** 2002. Functional analysis of the *Bacillus subtilis* Zur regulon. J. Bacteriol. **184**:6508–6514.
32. **Gabriel SE, Helmann JD.** 2009. Contributions of Zur-controlled ribosomal proteins to growth under zinc starvation conditions. J. Bacteriol. **191**:6116–6122.
33. **Guerout-Fleury AM, Frandsen N, Stragier P.** 1996. Plasmids for ectopic integration in *Bacillus subtilis*. Gene **180**:57–61.
34. **Hakansson KO, Brugna M, Tasse L.** 2004. The three-dimensional structure of catalase from *Enterococcus faecalis*. Acta Crystallogr. D Biol. Crystallogr. **60**:1374–1380.
35. **Hartford OM, Dowds BC.** 1994. Isolation and characterization of a hydrogen peroxide resistant mutant of *Bacillus subtilis*. Microbiology **140**: 297–304.
36. **Hayashi K, Ohsawa T, Kobayashi K, Ogasawara N, Ogura M.** 2005. The H_2O_2 stress-responsive regulator PerR positively regulates *srfA* expression in *Bacillus subtilis*. J. Bacteriol. **187**:6659–6667.
37. **Heinemann IU, Jahn M, Jahn D.** 2008. The biochemistry of heme biosynthesis. Arch. Biochem. Biophys. **474**:238–251.
38. **Helmann JD, et al.** 2003. The global transcriptional response of *Bacillus subtilis* to peroxide stress is coordinated by three transcription factors. J. Bacteriol. **185**:243–253.
39. **Herbig AF, Helmann JD.** 2001. Roles of metal ions and hydrogen peroxide in modulating the interaction of the *Bacillus subtilis* PerR peroxide regulon repressor with operator DNA. Mol. Microbiol. **41**:849–859.
40. **Hillmann F, Fischer RJ, Saint-Prix F, Girbal L, Bahl H.** 2008. PerR acts as a switch for oxygen tolerance in the strict anaerobe *Clostridium acetobutylicum*. Mol. Microbiol. **68**:848–860.
41. **Horvath S.** 1968. Competence in *Bacillus subtilis* transformation system. J. Gen. Microbiol. **51**:85–95.
42. **Imlay JA.** 2008. Cellular defenses against superoxide and hydrogen peroxide. Annu. Rev. Biochem. **77**:755–776.
43. **Imlay JA.** 2003. Pathways of oxidative damage. Annu. Rev. Microbiol. **57**:395–418.
44. **Jacquamet L, et al.** 2009. Structural characterization of the active form of PerR: insights into the metal-induced activation of PerR and Fur proteins for DNA binding. Mol. Microbiol. **73**:20–31.
45. **Kwon SJ, de Boer AL, Petri R, Schmidt-Dannert C.** 2003. High-level production of porphyrins in metabolically engineered *Escherichia coli*: systematic extension of a pathway assembled from overexpressed genes involved in heme biosynthesis. Appl. Environ. Microbiol. **69**:4875–4883.
46. **Lee JW, Helmann JD.** 2006. Biochemical characterization of the struc-

tural Zn^{2+} site in the *Bacillus subtilis* peroxide sensor PerR. J. Biol. Chem. **281**:23567–23578.
47. **Lee JW, Helmann JD.** 2007. Functional specialization within the Fur family of metalloregulators. Biometals **20**:485–499.
48. **Leelakriangsak M, Kobayashi K, Zuber P.** 2007. Dual negative control of *spx* transcription initiation from the P3 promoter by repressors PerR and YodB in *Bacillus subtilis*. J. Bacteriol. **189**:1736–1744.
49. **Loewen PC, Switala J.** 1987. Purification and characterization of catalase-1 from *Bacillus subtilis*. Biochem. Cell Biol. **65**:939–947.
50. **Ma Z, Gabriel SE, Helmann JD.** 2011. Sequential binding and sensing of Zn(II) by *Bacillus subtilis* Zur. Nucleic Acids Res. **39**:9130–9138.
51. **Ma Z, Lee JW, Helmann JD.** 2011. Identification of altered function alleles that affect *Bacillus subtilis* PerR metal ion selectivity. Nucleic Acids Res. **39**:5036–5044.
52. **May JJ, Wendrich TM, Marahiel MA.** 2001. The *dhb* operon of *Bacillus subtilis* encodes the biosynthetic template for the catecholic siderophore 2,3-dihydroxybenzoate-glycine-threonine trimeric ester bacillibactin. J. Biol. Chem. **276**:7209–7217.
53. **McCabe BC, Gollnick P.** 2004. Cellular levels of *trp* RNA-binding attenuation protein in *Bacillus subtilis*. J. Bacteriol. **186**:5157–5159.
54. **Miethke M, et al.** 2006. Ferri-bacillibactin uptake and hydrolysis in *Bacillus subtilis*. Mol. Microbiol. **61**:1413–1427.
55. **Miller JH.** 1972. Experiments in molecular genetics, p 352–355. Cold Spring Harbor Laboratory, Cold Spring Harbor, NY.
56. **Moore CM, Helmann JD.** 2005. Metal ion homeostasis in *Bacillus subtilis*. Curr. Opin. Microbiol. **8**:188–195.
57. **Nairz M, Schroll A, Sonnweber T, Weiss G.** 2010. The struggle for iron-a metal at the host-pathogen interface. Cell. Microbiol. **12**:1691–1702.
58. **Ollinger J, Song KB, Antelmann H, Hecker M, Helmann JD.** 2006. Role of the Fur regulon in iron transport in *Bacillus subtilis*. J. Bacteriol. **188**:3664–3673.
59. **Olsson U, Billberg A, Sjovall S, Al-Karadaghi S, Hansson M.** 2002. In vivo and in vitro studies of *Bacillus subtilis* ferrochelatase mutants suggest substrate channeling in the heme biosynthesis pathway. J. Bacteriol. **184**:4018–4024.
60. **Peters WJ, Warren RA.** 1970. The accumulation of phenolic acids and coproporphyrin by iron-deficient cultures of *Bacillus subtilis*. Can. J. Microbiol. **16**:1179–1185.
61. **Quisel JD, Burkholder WF, Grossman AD.** 2001. In vivo effects of sporulation kinases on mutant Spo0A proteins in *Bacillus subtilis*. J. Bacteriol. **183**:6573–6578.
62. **Rea R, Hill C, Gahan CG.** 2005. *Listeria monocytogenes* PerR mutants display a small-colony phenotype, increased sensitivity to hydrogen peroxide, and significantly reduced murine virulence. Appl. Environ. Microbiol. **71**:8314–8322.
63. **Sambrook J, Fritsch EF, Maniatis T.** 1990. Molecular cloning: a laboratory manual, 2nd ed. Cold Spring Harbor Press, Cold Spring Harbor, NY.
64. **Vagner V, Dervyn E, Ehrlich SD.** 1998. A vector for systematic gene inactivation in *Bacillus subtilis*. Microbiology **144**:3097–3104.
65. **Watnick PI, Eto T, Takahashi H, Calderwood SB.** 1997. Purification of *Vibrio cholerae* Fur and estimation of its intracellular abundance by antibody sandwich enzyme-linked immunosorbent assay. J. Bacteriol. **179**:243–247.
66. **Zheng M, Doan B, Schneider TD, Storz G.** 1999. OxyR and SoxRS regulation of *fur*. J. Bacteriol. **181**:4639–4643.
67. **Zuber P.** 2009. Management of oxidative stress in Bacillus. Annu. Rev. Microbiol. **63**:575–597.
68. **Zuber P, Losick R.** 1987. Role of AbrB in Spo0A- and Spo0B-dependent utilization of a sporulation promoter in *Bacillus subtilis*. J. Bacteriol. **169**:2223–2230.